University of Kragujevac
Serbia

SEECCM 06

First South-East European Conference on Computational Mechanics

PROCEEDINGS

Editors
Miloš Kojić and Manolis Papadrakakis

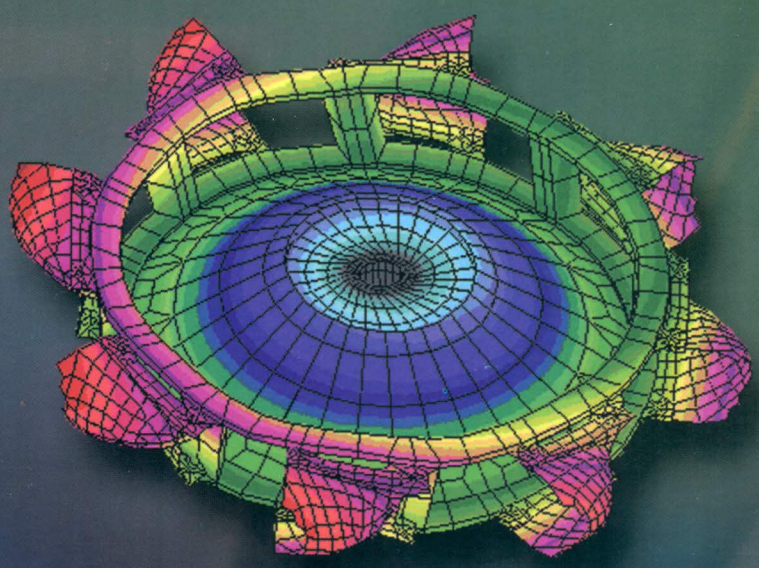

28-30 June 2006 Kragujevac
Serbia

ORGANIZING BOARD

Conference Chairmen

Manolis Papadrakakis, Greece
Milos Kojic, Serbia

Scientific Committee

Nikos Aravas, Greece
George Belgiu, Romania
Dimitris Beskos, Greece
Drago Blagojevic, Bosnia and Hercegovina
Radu Bogdan, Romania
Andreas Boudouvis, Greece
Livija Cveticanin, Serbia
Vlatko Dolocek, Bosnia and Hercegovina
Eugen Ghita, Romania
Matjaz Hribersek, Slovenia
Adnan Ibrahimbegovic, France
Boris Jeremic, USA
Aleksandar Jovanovic, Germany
Spyros Karamanos, Greece
Vlado Lubarda, USA
Nikos Makris, Greece
Emil Manoah, Bulgaria
Goran Markovski, FYR Macedonia
Dunja Martinovic, Bosnia and Hercegovina
Franjo Matejicek, Croatia
Hemann Matthies, Germany
Srboljub Mijailovic, USA
Dubravka Mijuca, Serbia
Borivoje Mikic, USA
Peter Minev, Canada
Golubka Necevska-Cvetanovska, FYR Macedonia
Aleksandar Ostrogorsky, USA
Milija Pavlovic, England
Cvetanka Popovska, FYR Macedonia
Stefan Radev, Bulgaria
Zoran Rajlic, Bosnia and Hercegovina
Zoran Ren, Slovenia
Aleksandar Sedmak, Serbia
Miodrag Sekulovic, Serbia
Leopold Skerget, Slovenia
Jurica Soric, Croatia
Constantinos Spiliopoulos, Greece
Dimitrije Stamenovic, USA
Milenko Stegic, Croatia
Demosthenis Talaslidis, Greece
Eustathios Theotokoglou, Greece
George Tsamasphyros, Greece
Rade Vignjevic, England
Miroslav Zivkovic, Serbia

Organizing Committee

President: Milos Djuran,
Rector of University of Kragujevac

Secretary: Nenad Filipovic

Members:

Radovan Slavkovic
Miroslav Zivkovic
Boban Stojanovic
Milos Ivanovic
Vladimir Rankovic
Miroljub Krstic
Lazar Otasevic
Mileta Nedeljkovic
Ivo Vlastelica
Gordana Jovicic
Gordana Bogdanovic
Snezana Vulovic
Bojane Medjo

First South-East European Conference on Computational Mechanics, SEECCM-06
(M. Kojić, M. Papadrakakis (Eds.))
June 28-30, 2006, Kragujevac, Serbia
University of Kragujevac

Dropwise Condensation Used In Mechanical Vapor Compression Desalination Plant – Computational Model

N. Lukić[1], A. Leipertz[2], A. Fröba[2], L. Diezel[2]

[1] Faculty of ME, Kragujevac, SCG
e-mail: lukic@kg.ac.yu
[2] Department Engineering Thermodynamics, Friedrich-Alexander University, Erlangen-Nürnberg, Germany

Abstract

Using ion-implanted metallic surfaces to induce a dropwise condensation improves the convective heat transfer coefficient significantly. The process of thermal desalination process, especially mechanical vapor compression (MVC) could be more effective by applying ion-implantation technology. This paper points to a possible reduction of heat transfer area of the main heat exchanger, using the specific MVC process. We showed in a selected MVC plant simulation model (mathematical model and developed software), that replacing filmwise by dropwise condensation could improve both main convective heat transfer processes (condensation and evaporation) by increasing the condensation heat transfer coefficient as well as the heat flux. For assumed improvement factor of dropwise condensation, comparing with filmwise condensation with the same MVC plant capacity, the reduction of main heat exchanger area is between 40% and 45%. The best improvement effect shows about a 10°C condensation-evaporation temperature difference.

Key words: desalination, mechanical vapor compression, dropwise condensation

1. Introduction

Although we are surrounded by huge amount of water, a drinking water shortage becomes the world problem. Whence the biggest part of this amount is saline water, one of logical solution is desalination. There are two main desalination techniques: membrane and evaporation. In other words, we can use non-thermal or thermal process to obtain drinking water. Membrane technique as reverse osmosis (RO) is generally a low energy and low price but also low product quality desalination method.

Point of our interest is evaporation technique. Depends on desalination plant capacity, availability of steam sources, electrical energy prices and specific demands, different thermal process can be used. Those are mainly: Multi-Stage Flash distillation (MSF), Multi Effect Distillation (MED), Thermal and Mechanical Vapor Compression (TVC and MVC) [1]. Thermal techniques that require an external steam source (MSF, MED, TVC) can be improved by cogeneration process [5]. Because an evaporation of saline (sea) water is obligatory for defined techniques, a problem of energy efficiency is dominant. In other words the condensation latent heat of product water should be used to provoke evaporation of saline water in condition when the temperature level of produced vapor is not enough to enable stabile evaporation of saline water. Recovering energy ratio of mechanical vapor compression (MVC) technique (vapor is pressurized by compressor) can be very high but a spent energy is very expensive electrical energy. This is one stage desalination method for smaller product capacities (up to 3000 m^3/day). In MVC plants, rang of the specific energy consumption is mostly 7-12 kWh/m^3. Higher energy efficiency means a smaller evaporation-condensation side temperature difference and bigger demanded heat transfer area. There is chance for scientists to achieve an optimum thermal desalination scenario.

Many approaches to mentioned scenario are recorded. In [2], the realized MVC desalination plants have given a good production results but because small evaporation-condensation side temperature difference (dt=3-4°C) the used plate one-phase and tube evaporation-condensation heat exchangers are huge (heat transfer area of he_{ec}=2598 m^2). In [3] the classic MVC model was considered by simple LMTD calculation method for heat transfer phenomena. In Vapor compression plant (VC), a dominant centrifugal compressor and its significant consumption of electrical energy can be replaced by classic heat pump cycle [7], [4], [6], absorption heat pump cycle [4], thermal vapor compression (TVC), using ejector and external steam source [4].

Farther, in heat pump cycle energy consumption can be reduced using solar energy for working fluid evaporation (delimited from water cycle) [6]. All mentioned desalination plant model or installation decrease specific energy consumption (exception is TVC) very effective but problem is its limited production capacity often on insufficient level. On other side a centrifugal compressor can be driven by wind energy [8], [9] but beside small production capacity, a stabile plant functioning is basic problem of this concept. The aim of all presented methods is energy efficiency increasing by reduction of MVC demanded driving electrical energy.

Other (our) approach is based on improvement of MVC plant heat transfer coefficient. Plate heat exchanger (PHE) concept provides high heat transfer coefficient (very low turbulent transition Re number) and relative small pressure drop for any heat transfer scenario (one-phase, evaporation, condensation) [10]. On other side filmwise condensation (FWC) can be converted to more effective dropwise condensation (DWC) using ion implanted metallic surface. This means significant multiplied condensation heat transfer coefficient depending on heat transfer conditions [12], [13]. Probably, using on the same way treated metallic surface, it can also improve evaporation heat transfer coefficient but it needs more investigation. In [11] it was described the successful inhibition of scaling process in desalination plant using ion implanted metallic surface but there same improvement of evaporation heat transfer coefficient can be found. Further it will be presented the designed MVC mathematical model (based on PHE and DWC) and the obtained results.

2. MVC Mathematical model

2.1 The assumed desalination plant

The assumed mechanical vapor compression desalination plant (MVC) is consisted of two one-phase plate heat exchangers (parallel connection) and one main evaporation-condensation plate heat exchanger and other necessary equipments. The schematic diagram of MVC one-phase PHE parallel connection is shown on figure 1. There was also considering the one-phase PHE serial connection but this calculation model has given significantly low heat transfer results.

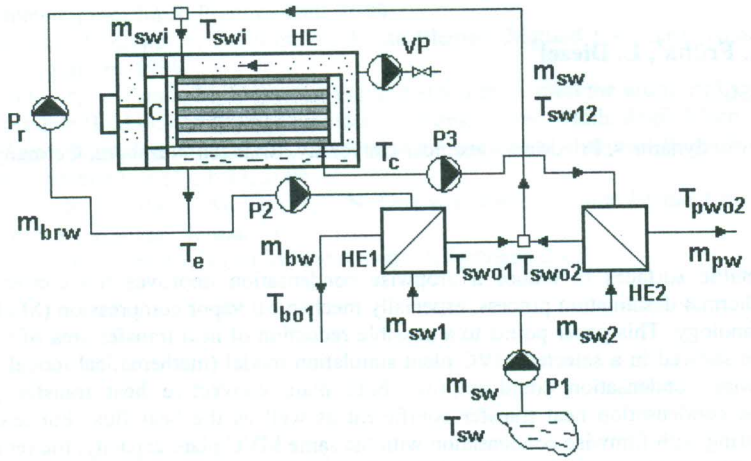

Figure 1 Schematic diagram of the MVC desalination plant

There are: HE1 - the brine heat exchanger, HE2 - the product water heat exchanger, HE - the main (evaporation-condensation) heat exchanger, P1,P2,P3,P_r - pumps, VP - vacuum pump, C - compressor, m_{pw} - product water mass flow rate (kg/s); m_{sw} - sea water mass flow rate (kg/s); m_{bw} - brine mass flow rate (kg/s); m_{bwr} - recirculation brine mass flow rate (kg/s); m_{sw1} - sea water mass flow rate throughout HE1 (kg/s); m_{sw2} - sea water mass flow rate throughout HE2 (kg/s); m_{swi} - sea water mass flow rate throughout main heat exchanger (HE) (kg/s); t_{sw} - temperature of environmental sea water (°C); t_e - evaporation temperature (°C); t_c - condensation temperature (°C); t_{bo1} - HE1 outlet temperature of brine (°C); t_{pwo2} - HE2 outlet temperature of product water (°C); t_{swo1} - HE1 outlet temperature of sea water (°C); t_{swo2} - HE2 outlet temperature of sea water (°C); t_{swi} - HE inlet temperature of sea water (°C); t_{swo12} - outlet temperature of sea water after mixing HE1 and HE2 flows (°C).

During real functioning of MVC plant, instead the water evaporation temperature, t_e (°C), the increased saline water evaporation temperature, t_{be} (°C) exists. This temperature is function of pure water evaporation temperature and salt percent s_{p100} (%) or salt ratio s_p (-), $t_{be}=f(te,s_{p100})$.

The MVC mathematical model can be divided on three structural parts: 1. The one-phase PHE mathematical model; 2. The commpresor mathematical model; 3. The two-phase main heat exchanger (HE_m) mathematical model.

2.2 The one-phase plate heat exchanger mathematical model

According to the shown figure 1 (PHE parallel connection), mass and energy equations, the one-phase parallel connection mathematical model can be expressed. Convective heat transfer coefficients of one-phase plate heat exchangers HE1 and HE2 are calculated according to [14]. Warm outlet flows of brine and product water from HE1 and HE2 present the MVC plant heat losses:

$$Q_{l1} = m_{bw} \cdot c_{bw} \cdot (t_{bo1} - t_{sw}) , \tag{1}$$

$$Q_{l2} = m_{pw} \cdot c_w \cdot (t_{pwo2} - t_{sw}) . \tag{2}$$

There are: Q_{l1} - heat loss of heat exchanger HE1 (kW); Q_{l2} - heat loss of heat exchanger HE2 (kW); c_{bw} – saline water heat capacity, function of temperature and salt percent (kJ/kgK); c_w – water heat capacity, function of temperature (kJ/kgK). The MVC heat losses must be equal with MVC heat gain, the real compressor power, P_{rc} (kW):

$$P_{rc} = Q_{l1} + Q_{l2} , \tag{3}$$

and according to this equation, the one-phase heat transfer areas of HE1 and HE2 should be adjusted (changing of N_{o1},N_{o2},w_1,w_2,h_1,h_2) to real values.

Obviously, smaller MVC heat losses mean smaller the MVC compressor power and smaller electrical energy consumption. This directly depends on the HE1 and HE2 functioning.

The size of this paper does not allow detailed mathematical model showing. More information can be found in [25].

2.3 The compressor mathematical model

The real compressor power is calculated as:

$$l_{tcr} = (h_{cisv} - h_{ebsv}) / \eta_{ic} ; \quad P_{rc} = m_{pw} \cdot l_{tcr} . \tag{4}$$

There are: l_{tcr} - compressor real technical work (kJ/kg); h_{ebsv} - compressor inlet vapor enthalpy, superheated vapor enthalpy, $h_{ebsv}=f(p_e,t_{be})$ at water evaporation pressure p_e (MPa)=$f(t_e)$ and saline water evaporation temperature t_{be} ($t_{be}>t_e$) (kJ/kg). This enthalpy is bigger than saturated vapor enthalpy at temperature t_e.; h_{cisv} - isentropic compressor outlet vapor enthalpy, superheated vapor enthalpy, $h_{cisv}=f(p_c,s_{ebsv})$ at water condensation pressure p_c (MPa)=$f(t_c)$ and superheated vapor entropy, $s_{ebsv}=f(p_e,t_{be})$ (kJ/kg); η_{ic} - isentropic compressor efficiency (assumed value) (-). The real compressor outlet vapor enthalpy is calculated as:

$$h_{crsv} = h_{ebsv} + l_{tcr} \,. \tag{5}$$

The compressor outlet vapor temperature t_{crsv} (°C)=$f(p_c,h_{crsv})$ is function of condensation pressure, p_c and real compressor outlet vapor enthalpy, h_{crsv}. For computer calculation of saturated and superheated vapor properties, the high precise equations are used.

The specific compressor energy consumption (≈MVC energy consumption), E_{sc} (kwh/m^3) per m^3 of product water is calculated as:

$$E_{sc} = 24 \cdot P_{rc} \, Q_{MVC} \,. \tag{6}$$

There is: Q_{MVC} - capacity of MVC plant (m^3/day). The efficiency factor of MVC plant, F_e (-) is calculated as:

$$F_e = r_{te} / l_{tcr} \,. \tag{7}$$

There is: r_{te} - water evaporation latent heat at evaporation pressure (kJ/kg).

2.4 The evaporation-condensation plate heat exchanger (HE_m) mathematical model

Two stream cases are possible in HE_m: parallel flow HE_m and counter flow HE_m. The parallel flow HE_m has three possible heat transfer zones (Fig. 2 and 3): vapor-brine heat transfer zone (HE_m inlet); vapor-evaporation heat transfer zone or brine-condensation heat transfer zone and evaporation-condensation heat transfer zone (main heat transfer area).

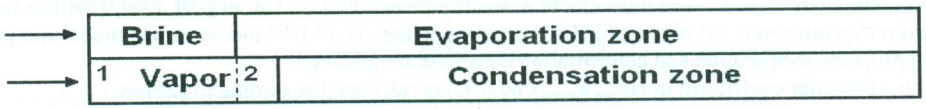

Figure 2 Schematic diagram of parallel flow HE_m, case $Q_{vbc}>Q_{wae}$

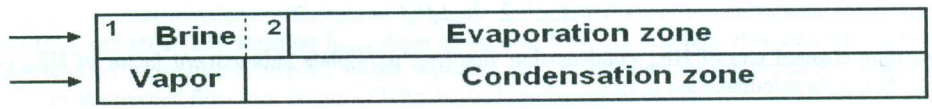

Figure 3 Schematic diagram of parallel flow HE_m, case $Q_{vbc}<Q_{wae}$

There Q_{vbc} (kW) presents the heat power needed to achieve the saturated vapor state (vapor cooling to start of condensation) and Q_{wae} (kW) presents the heat power needed to achieve the saturated brine liquid state (brine heating to start of evaporation). The heat power Q_{vbc} and Q_{wae} are calculated as:

$$Q_{wae} = m_{swi} \cdot c_{bw} \cdot (t_{be} - t_{swi}) \,, \tag{8}$$

$$Q_{vbc} = m_{pw} \cdot (h_{crsv} - h_c) \,. \tag{9}$$

There is h_c - saturated enthalpy at condensation temperature (kJ/kg). The counter flow HE_m has three possible heat transfer zones (Fig. 4): vapor-evaporation heat transfer zone (HE_m inlet); brine-condensation heat transfer zone (HE_m outlet) and evaporation-condensation heat transfer zone (main heat transfer area).

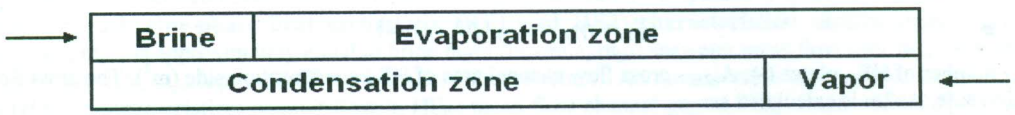

Figure 4 Schematic diagram of counter flow HE_m

The real HE_m inlet temperature of seawater, t_{swi} is calculated using the heat power equality of HE_m evaporation and condensation side:

$$\begin{aligned} &m_{swi} \cdot c_{bw} \cdot (t_{be} - t_{swi}) + m_{pw} \cdot r_{te} = m_{pw} \cdot (h_{crsv} - h_c) + m_{pw} \cdot r_{te} \;\Rightarrow \\ &t_{swi} = t_{be} - m_{pw} \cdot (h_{crsv} - h_c + r_{tc} - r_{te}) / (m_{swi} \cdot c_{bw}) \end{aligned} \tag{10}$$

There is r_{tc} - water condensation latent heat at condensation pressure (kJ/kg). According to the real temperature, tswi, the one-phase heat exchanger areas should be adjusted (connect. with equation 3).

The heat transfer equations in HE_m are:

$$Q_{hem} = A_{hem} \cdot U_{hem} \cdot \Delta t_{mm}; Q_{hem1} = A_{hem1} \cdot U_{hem1} \cdot \Delta t_{mm1}; Q_{hem2} = A_{hem2} \cdot U_{hem2} \cdot \Delta t_{mm2} \quad (11)$$

There are: Q_{hem} - heat power of evaporation-condensation HE_m area (kW); Q_{hem1} - heat power of inlet HE_m area (kW); Q_{hem2} - heat power of outlet (or second inlet) HE_m area (kW); A_{hem} - heat transfer area of evaporation-condensation HE_m zone (m^2); A_{hem1} - heat transfer area of inlet HE_m zone (m^2); A_{hem2} - heat transfer area of outlet (or second inlet) HE_m zone (m^2); U_{hem} - total heat transfer coefficient of evaporation-condensation HE_m area (W/m^2K); U_{hem1} - total heat transfer coefficient of inlet HE_m area (W/m^2K); U_{hem2} - total heat transfer coefficient of outlet (or second inlet) HE_m area (W/m^2K); Δt_{mm} - mean logarithmic tem. difference of evaporation-condensation HE_m area (°C); Δt_{mm1} - mean logarithmic temperature difference of inlet HE_m area (°C); Δt_{mm2} - mean logarithmic tem. difference of outlet (or second inlet) HE_m area (°C).

The size of this paper does not allow detailed mathematical model showing. Only the calculation of U_{hem} (the most important total heat transfer coefficient) will be shown. More information can be found in [25].

According to equation (11) the total heat transfer coefficients U_{hem} are:

$$U_{hem} = 1 \Big/ \left(\frac{1}{if_e \cdot h_{mevp}} + \frac{\delta_m}{\lambda_m} + \frac{1}{if_c \cdot h_{mcon}} \right) \Rightarrow all \quad three \quad cases, \quad (12)$$

There are: h_{mevp} - evaporation heat transfer coefficient in HE_m (W/m^2K); h_{mcon} - condensation heat transfer coefficient in HE_m (W/m^2K); δ_m - thickness of HE_m plate (m); λ_m - thermal conductivity of HE_m plate (W/mK); if_e - improvement factor of dropwise evaporation (-); if_c - improvement factor of dropwise condensation (-).

The choosing of appropriate equations for condensation and evaporation heat transfer coefficient calculation in small channels as PHE flow area is very difficult problem. For example, in [22] can be found that eleven correlations for conventional and narrow-channel boiling predicted the data poorly, ranging form 250% average over-prediction to 70% average under-prediction. In [15]-[19], [23], can be fount more evaporation predictions of water and refrigerants in small pipe and PHE. Also, in [20], [21], [24] can be found condensation predictions of water and refrigerants in small pipe and PHE. According to assumed MVC mathematical model and presented literature, in further text, the most appropriate evaporation and condensation equations are assumed.

The condensation heat transfer coefficient in HE_m, h_{mcon} (W/m^2K) is calculated according to [24] as:

$$h_{mcon} = Nu_{mcon} \cdot \lambda_w / d_{e2m}. \quad (13)$$

There are: d_{e2m} - equivalent diameter of HE_m condensation side (m); Nu_{mcon} - condensation Nusselt number in HE_m (-); λ_m - thermal conductivity of HE_m plate (W/mK). The equivalent diameter of HE_m condensation side, d_{e2m} is calculated as:

$$d_{e2m} = 2 \cdot b_{2m} / \mu_m. \quad (14)$$

There are: b_{2m} - mean flow channel gap of HE_m condensation side (m); μ_m - plate enlargement factor of HE_m (-). The condensation Nusselt number in HE_m, Nu_{mcon} is calculated as:

$$Nu_{bw} = C \cdot \mathrm{Re}_{q2m}^{m} \cdot \mathrm{Pr}_w^{0.33}. \quad (15)$$

There are: C, m - constants (-) that depend on β_m (°), plate chevron angle of HE_m as C=3.77; m=0.43; when β_m=60° and C=0.325; m=0.62; when β_m=30° (two fixed plate chevron angle option); Re_{q2m} - hydraulic Reynolds number of HE_m condensation side (-). The hydraulic Reynolds number of HE_m condensation side, Re_{q2m} is calculated as:

$$\mathrm{Re}_{q2m} = G_{eq2m} \cdot d_{e2m} / \eta_w. \quad (16)$$

There is G_{eq2m} - modified equivalent mass flux of HE_m condensation side (kg/m^2s). The modified equivalent mass flux of HE_m condensation side, G_{eq2m} is calculated as:

$$G_{eq2m} = G_{2m} \cdot \left[1 - x_{2m} + x_{2m} \cdot (\rho_w / \rho_v)^k \right]. \quad (17)$$

There are: k - constant (-) that depends on β_m as k=0.14; when β_m=60° and k=0.4; when β_m=30°; G_{2m} - mass flux of HE_m condensation side (kg/m^2s); β_m – plate chevron angle in HE_m (°); x_{2m} - mean vapor quality of HE_m condensation side, x_{2m}=0.5 (condensation starts at x=1 and ends at x=0) (-); ρ_v - vapor density at corresponding (condensation) temperature (kg/m^3). The mass flux of HE_m condensation side, G_{2m} is calculated as:

$$G_{2m} = m_{pw} / [A_{x2m} (N_{om} - 1)/2]. \quad (18)$$

There are: N_{om} - number of HE_m plates (-); A_{x2m} - cross flow channel area of HE_m condensation side (m^2). The cross flow channel area of HE_m condensation side, Ax2m is calculated as:

$$A_{x2m} = b_{2m} \cdot w_m. \quad (19)$$

There is: w_m - effective width of HE_m plate (m). The evaporation heat transfer coefficient in HE_m, h_{mevp} (W/m^2K) is calculated according to [23] as:

$$h_{mevp} = E_{1m} \cdot h_{11m} + S_{1m} \cdot h_{pool}. \quad (20)$$

There are: E_{1m}, S_{1m} - enhancement and suppression factors (-); h_{11m} - evaporation convective heat transfer coefficient (W/m^2K); h_{pool} - evaporation nucleate boiling heat transfer coefficient (W/m^2K).

The enhancement and suppression factor, E_{1m} is calculated as:

$$E_{1m} = 1 + 24000 \cdot Bo_{1m}^{1.16} + 1.37 \cdot (1/X_{tt1m})^{0.86}. \quad (21)$$

There are: Bo_{1m} - Boiling number of HE_m evaporation side (-); X_{tt1m} - Martinelli parameter of HE_m evaporation side (-). The boiling number of HE_m evaporation side, Bo_{1m} is calculated as:

$$Bo_{1m} = q_{1m} / G_{1m} \cdot r_{te} \,. \tag{22}$$

There are: q_{1m} - heat flux of HE_m evaporation side (W/m^2); G_{1m} - mass flux of HE_m evaporation side (kg/m^{2}s). The mass flux, G_{1m} is calculated according to equation (18), using variables: N_{om}, m_{swi} and A_{x1m}, there the cross flow channel area of HE_m evaporation side, A_{x1m} (m^2) is calculated according to equation (19), using variables: b_{1m} and w_m, there b_{1m} (m) is mean flow channel gap of HE_m evaporation side. The Martinelli parameter of HE_m evaporation side, X_{tt1m} is calculated as:

$$X_{tt1m} = ((1-x_{1m})/x_{1m})^{0.9} \cdot (\rho_v / \rho_{bw})^{0.5} \cdot (\eta_{bw} / \eta_v)^{0.1} \,. \tag{23}$$

There are: x_{1m} - mean vapor quality of HE_m evap. side (evaporation starts at x=0 and ends at $x=m_{pw}/m_{swi}$) (-); η_v - vapor dynamic viscosity at corresponding (evaporation) temperature (Pa·s). The enhancement and suppression factor, S_{1m} is calculated as:

$$S_{1m} = \left(1 + 1.15e-6 \cdot E_{1m}^2 \cdot \mathrm{Re}_{l1m}^{1.17}\right)^{-1} \,. \tag{24}$$

There is Re_{l1m} - liquid Reynolds number of HE_m evaporation side (-). The liquid Reynolds number of HE_m evaporation side, Re_{l1m} is calculated as:

$$\mathrm{Re}_{l1m} = (1-x_{1m}) \cdot G_{1m} \cdot d_{e1m} / \eta_{bw} \,. \tag{25}$$

There is d_{e1m} - equivalent diameter of HE_m evaporation side (m).

The equivalent diameter of HE_m condensation side, d_{e1m} is calculated according to equation (14), using variables: b_{1m} and μ_m, there b_{1m} (m) is mean flow channel gap of HE_m evaporation side.

The evaporation convective heat transfer coefficient, h_{l1m} is calculated as:

$$h_{l1m} = 0.023 \cdot \mathrm{Re}_{l1m}^{0.8} \cdot \mathrm{Pr}_{bw}^{0.4} \cdot (\lambda_{bw} / d_{e1m}) \tag{26}$$

The evaporation nucleate boiling heat transfer coefficient, h_{pool} is calculated as:

$$h_{pool} = 55 \cdot p_{r1m}^{0.12} \cdot (-\log_{10} p_{r1m})^{-0.55} \cdot M^{-0.5} \cdot q_{1m}^{0.67} \,. \tag{27}$$

There are: p_{r1m} - relative evaporation pressure, $p_{r1m}=p_e/p_c$ (-), there pc is critical water pressure, p_c=22.089 MPa; M - molecular weight of water (kg/kmol), M=18. kg/kmol. The presented evaporation equations are valid for $2000<Re_{l1m}<12000$ and $0.0002<Bo_{1m}<0.002$.

The one-phase convective heat transfer coefficients of brine and superheated vapor are calculated according to equations for one-phase heat exchangers HE1 and HE2 [25]. Because h_{mevp} depends on heat flux, q_{1m} and heat flux depends on evaporation heat transfer coefficient, h_{mevp}, and iteration procedure is needed. When equation (10) is satisfied by the predicted heat flux value, the iteration procedure is finished. Then the needed flow path length of HE_m, h_m (m) can be calculated as:

$$A_{mtot} = A_{hem} + A_{hem1} + A_{hem2} = \frac{Q_{hem}}{U_{hem} \cdot \Delta t_{mm}} + \frac{Q_{hem1}}{U_{hem1} \cdot \Delta t_{mm1}} + \frac{Q_{hem2}}{U_{hem2} \cdot \Delta t_{mm2}} \,, \tag{28}$$

$$h_m = A_{mtol} / (N_{om} - 2) \cdot w_m \,. \tag{29}$$

There is A_{mtot} - total HE_m heat transfer area (m^2) and h_m - flow path length in HE_m (m).

3. Results and discussion

3.1 The start values of MVC mathematical model

Described MVC plant mathematical model was taken from MVC1 software [25]. After this step, the chosen MVC plant model and simulation conditions were assumed. In further text, the used MVC characteristics and simulation conditions are described (constant simulation values):

Seawater characteristics: salt percent, s_{p100}=3%; environmental temperature, t_{sw}=20°C. **General MVC plant characteristics:** product/seawater ratio, α=0.3; recirculation brine flow ratio, α_b=0; condensation temperature, t_c=80°C. **Compressor characteristics:** isentropic efficiency, η_{ic}=0.8. **One-phase heat exchangers (HE1 and HE2) characteristics:** parallel connection HE1 and HE2; seawater mass flow rate, m_{sw1} is approximately equal to brine mass flow rate, m_{bw}; seawater mass flow rate, m_{sw2} is approximately equal to product water mass flow rate, m_{pw} (optimal effect of parallel HE connection). Additional information can be found in [25]. **Two-phase heat exchangers (HE_m) characteristics:** counter flow in HE_m; mean flow channel gap of HE_m evaporation side = mean flow channel gap of HE_m condensation side, b_{1m}= b_{2m}=6 mm; thickness of HE_m plate, δ_m=0.6 mm; enlargement factor of HE_m plate, μ_m=1.17; chevron angle of HE_m plate, β_m=60°; thermal conductivity of HE_m plate, λ_m= 20 W/mK (the material of plates is stainless steel ion-implanted or not); the improvement factor of evaporation, if_e=1 (filmwise condensation). **Variable simulation values:** Same characteristics and conditions of MVC model have taken two to five different values. **General MVC plant characteristics:** evaporation temperature, t_e=76°C, 73°C, 70°C, 67°C and 64°C (condensation-evaporation temperature difference, t_c-t_e=4°C, 7°C, 10°C, 13°C and 16°C); MVC plant capacity, Q_{MVC}=100 m^3/day, 200 m^3/day, 300 m^3/day. **Two-phase heat exchangers (HE_m) characteristics:** values of effective width of plate and number of plates depend on chosen plant capacity (Q_{MVC}) according to scheme: for Q_{MVC}=100 m^3/day: effective width of HE_m plate, w_m=0.4 m; number of HE_m plates, N_{om}=71; for Q_{MVC}=200 m^3/day: w_m=0.5 m; N_{om}=91; for Q_{MVC}=300 m^3/day: w_m=0.6 m; N_{om}=101; All defined values were adjusted to a evaporation liquid Reynolds number and evaporation boiling number range for validation of calculation data (see [23]) in evaporation side of HE_m ($2000<Re_{l1m}<12000$ and $0.0002<Bo_{1m}<0.002$). Two values of improvement factor of condensation, if_c are assumed: if_c=1 for stainless steel plates (filmwise condensation) and if_c=5 for ion-implanted stainless steel plates (dropwise condensation).

Using values described in previous chapter, the planed simulation data were obtained.

3.2 Simulation results

Figure 5 shows the influence of temperature difference of condensation-evaporation side to the compressor power demanded, P_{rc} and specific electrical energy consumption of MVC plant, E_{sc}. The usual and recommended E_{sc} values are in range between 7 kWh/m^3 and 12 kWh/m^3 ([26]). This means that MVC plant operative range of c-e temperature difference, Δt_{mm} is placed between 4°C and 6°C, approximately. Certainly, under specific conditions the bigger specific electrical energy consumption can be acceptable ([27]). Usually, the electrical energy consumption is the biggest part of a MVC plant product water price. Good functioning of MVC plant under small c-e temperature difference demands an improvement of c-e heat transfer process.

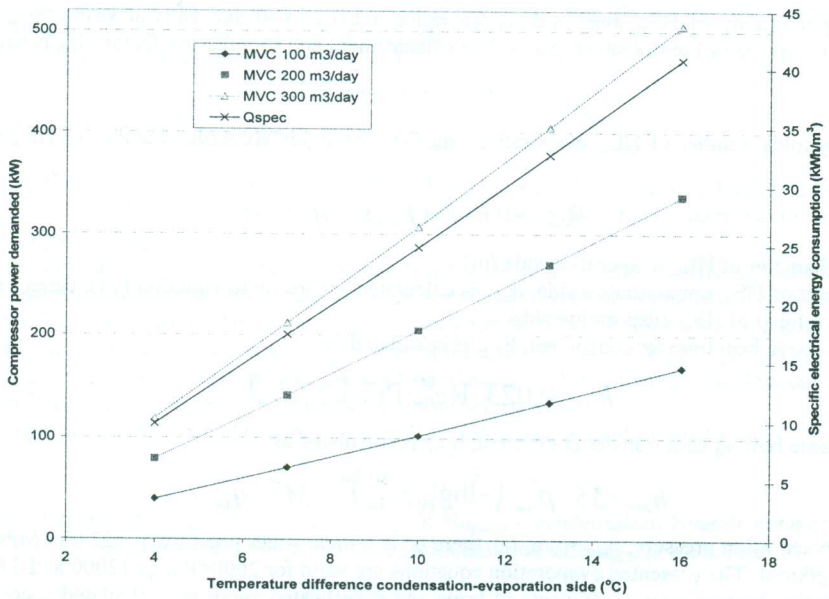

Fig. 5 The influence of temperature difference of condensation-evaporation side to the compressor power demanded and specific electrical energy consumption of MVC plant

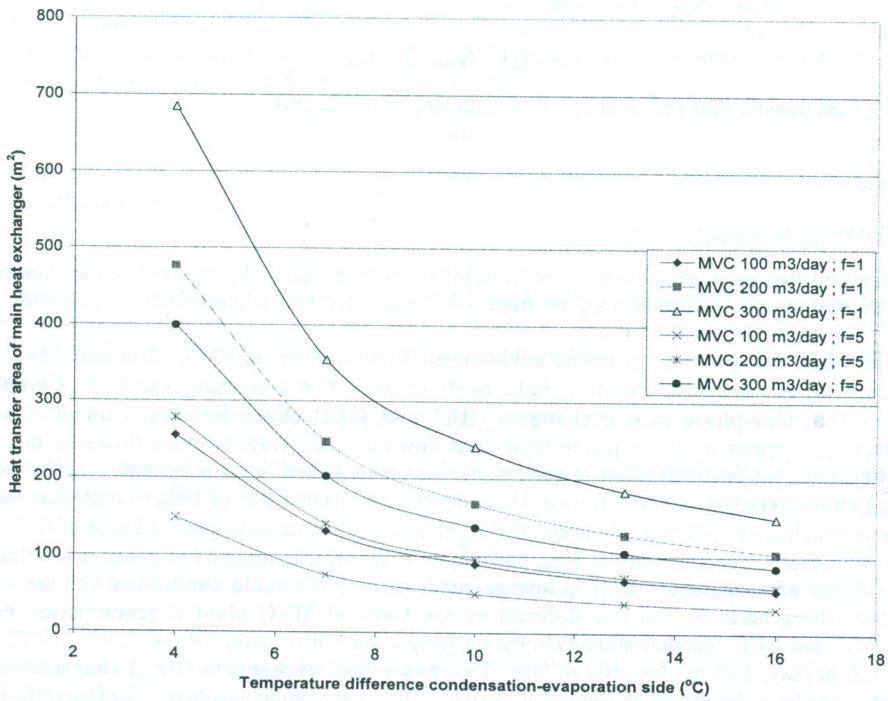

Fig. 6 The influence of temperature difference of condensation-evaporation side to the heat transfer area of MVC main heat exchanger for filmwise (if_c=1) and dropwise (if_c=5) condensation

Figure 7 shows the influence of temperature difference of condensation-evaporation side to the improvement effect of ion-implanted surfaces, $[A_{mtot}(if_c=1)- A_{mtot}(if_c=5)]/ A_{mtot}(if_c=1)$. For smaller MVC plant capacity the improvement effect is bigger. Generally, the relative reduction of A_{mtot} is placed between 40% and 45% for used simulation scenarios.

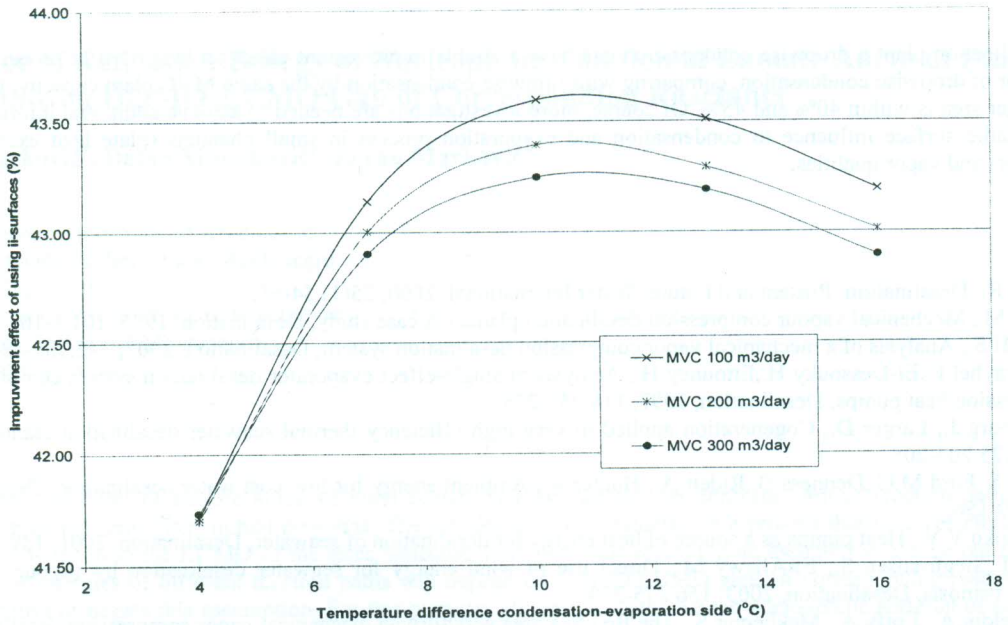

Fig. 7 The influence of temperature difference of condensation-evaporation side to the improvement effect of ion-implanted surfaces using in MVC main heat exchanger

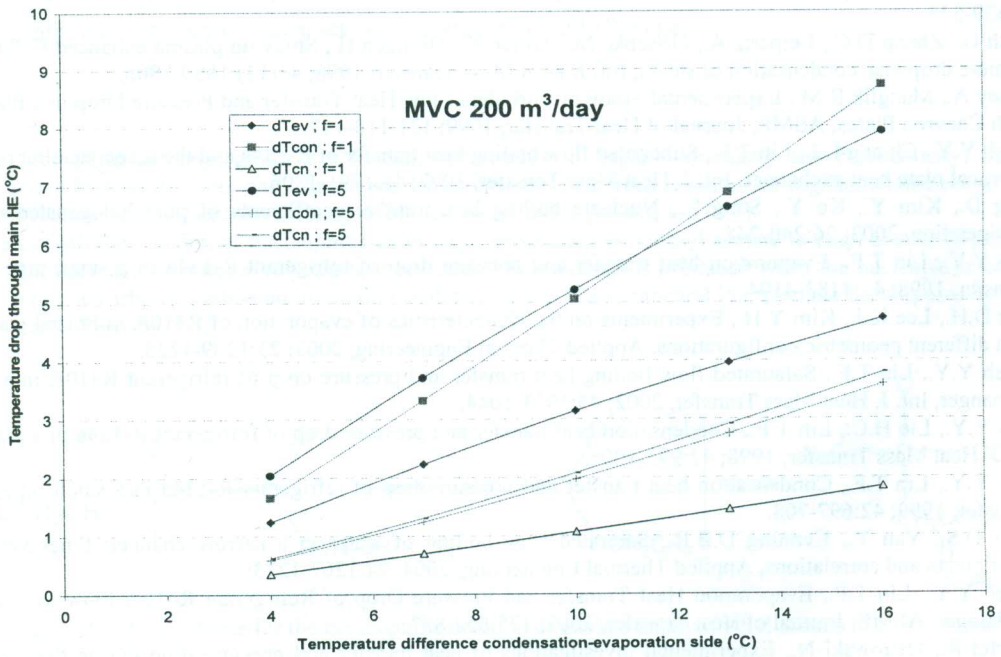

Fig. 8 The influence of temperature difference of condensation-evaporation side to the temperature drops through MVC main heat exchanger (evaporation, wall conduction and condensation) for filmwise ($if_c=1$) and dropwise ($if_c=5$) condensation and MVC plant capacity, $Q_{MVC}=200$ m^3/day

Total temperature difference between condensation and evaporation side in main heat exchanger (HE_m) is divided on particular temperature drops: evaporation, dT_{ev}, wall-conduction, dT_{cn} and condensation dT_{con}. The sum of those drops always has to be equal the total c-e temperature difference, Δt_{mm} (see Figure 8). A bigger temperature drop means a bigger thermal resistance. In case of filmwise condensation ($if_c=1$), condensation process makes the biggest thermal resistance in HE_m and on other side, wall-conduction thermal resistance (stainless still) is insignificant. In case of dropwise condensation ($if_c=5$), the most significant temperature drop is placed on evaporation side, while other two drops (dt_{cn} and dt_{con}) are very close. Evaporation temperature drop curves has different trend than other because the evaporation heat transfer coefficient directly depends on heat flux value (see equation (20)-(27)). In fact, improvement of

condensation process in HE_m has double effect. The dropwise condensation strongly influences on evaporation process, arising the evaporation heat flux and evaporation heat transfer coefficient.

4. Conclusion

In MVC desalination plant a dropwise condensation can have a double improvement effect on heat transfer process. For assumed improvement factor of dropwise condensation, comparing with filmwise condensation by the same MVC plant capacity, the reduction of main heat exchanger area is within 40% and 45%. Of course, more investigations are needed to achieve additional information about an ion-implanted metallic surface influence to condensation and evaporation process in small channels (plate heat exchangers), under variable Re-numbers and vapor qualities.

References

[1] Semiat R., Desalination: Present and Future, Water International, 2000; 25(1):54-65.
[2] Veza J.M., Mechanical vapour compression desalination plants - A case study, Desalination, 1995; 101:1-10.
[3] Aybar H.S., Analysis of a mechanical vapor compression desalination system, Desalination, 2002; 142:181-186.
[4] Al-Juwayhel F.,El-Dessouky H.,Ettouney H., Analysis of single-effect evaporator desalination system combined with vapor compression heat pumps, Desalination, 1997; 114:253-275.
[5] Gunzbourg J., Larger D., Cogeneration applied to very high efficiency thermal seawater desalination plants, Desalination, 1999; 125:203-208.
[6] Virk G.S.,Ford M.G.,Denness B.,Ridett A., Hunter A., Ambient energy for low-cost water desalination, Desalination, 2001; 137:149-156.
[7] Slasarenko V.V., Heat pumps as a source of heat energy for desalination of seawater, Desalination, 2001; 139:405-410.
[8] Witte T.,Siegfriedsen S., El-Allawy M., Direct use of wind energy for seawater desalination by vapour compression or reverse osmosis, Desalination, 2003; 156:275-279.
[9] Karameldin A., Lotfy A., Mekhemar S., The Red Sea area wind-driven mechanical vapor compression desalinataion system, Desalination, 2002; 153:47-53.
[10] Legorreta C., Hinge S., Tonner J., Lovato A., Plates-the next breakthrough in desalination, Desalination, 1999; 122:235-246.
[11] Muller-Steinhagen H., Zhao Q., Investigation of low fouling surface alloys made by ion implantation technology, Chemical Engineering Science, 1997; 52(19):3321-3332.
[12] Koch G., Kraft K., Leipertz A., Parameter stydy on the performance of dropwise condensation, Rev. Gen. Therm., 1998; 37:539-548.
[13] Koch G., Zhang D.C., Leipertz A., Grischke M., Trojan K., Dimigen H., Study on plasma enhanced CVD coated material to promote dropwise condensation of steam, Int. J. Heat Mass Transfer, 1998; 41(13):1899-1906.
[14] Muley A., Manglik R.M., Experimental Study of Turbulent Flow Heat Transfer and Pressure Drop in a Plate Heat Exchanger With Chevron Plates, ASME, Journal of Heat Transfer, 1999; 121:110-117.
[15] Hsieh Y.Y., Chiang L.J., Lin T.F., Subcooled flow boiling heat transfer of R-134a and the associated bubble characteristics in a vertical plate heat exchanger, Int. J. Heat Mass Transfer, 2002; 45:1791-1806.
[16] Jung D., Kim Y., Ko Y., Song K., Nucleate boiling heat transfer coefficients of pure halogenated refrigerants, Int. J. Refrigeration, 2003; 26:240-248.
[17] Yan Y.Y., Lin T.F., Evaporation heat transfer and pressure drop of refrigerant R-134a in a small pipe, Int. J. Heat Mass Transfer, 1998; 41:4183-4194.
[18] Han D.H., Lee K.J., Kim Y.H., Experiments on the characteristics of evaporation of R410A in brazed plate heat exchangers with different geometric configurations, Applied Thermal Engineering, 2003; 23:1209-1225.
[19] Hsieh Y.Y., Lin T.F., Sataurated flow boiling heat transfer and pressure drop of refrigerant R410A in a vertical plate heat exchanger, Int. J. Heat Mass Transfer, 2002; 45:1033-1044.
[20] Yan Y.Y., Lio H.C., Lin T.F., Condensation heat transfer and pressure drop of refrigerant R-134a in a plate heat exchanger, Int. J. Heat Mass Transfer, 1998; 42:993-1006.
[21] Yan Y.Y., Lin T.F., Condensation heat transfer and pressure drop of refrigerant R-134a in a small pipe, Int. J. Heat Mass Transfer, 1999; 42:697-708.
[22] Wen D.S., Yan Y., Kenning D.B.R., Saturated flow boiling of water in a narrow channel: time-averaged heat transfer coefficients and correlations, Applied Thermal Engineering, 2004; 24:1207-1223.
[23] Hsieh Y.Y., Lin T.F., Evaporation Heat Transfer nad Pressure Drop of Refrigerant R410A Flow in a Vertical Plate Heat Exchanger, ASME, Journal of Heat Transfer, 2003; 125:852-857.
[24] Wurfel R., Ostrowski N., Experimental investigations of heat transfer and pressure drop during the condensation process within plate heat exchangers of the herringbone-type, Int. J. Thermal Sciences, 2004; 43:59-68.
[25] Lukic N., Leipertz A., Diezel L., Froba A.P., Mechanical vapor compression desalination software MVC1, ESYTEC Energie und Systemtechnik GmbH Erlangen, 2004.
[26] Buros O.K., The ABCs of Desalting, Second Edition, International Desalination Association, Topsfield, Massachusetts, USA.
[27] Zyclodest, Product information, EnviTech GmbH, Mindelheim, Germany.